

Jet Substructure at HERA†

Claudia Glasman*
representing the ZEUS Collaboration

**Department of Physics and Astronomy, Kelvin Building,
University of Glasgow, Glasgow, G12 8QQ, UK*

Abstract. Measurements of jet shapes and subjet multiplicities in photoproduction performed by ZEUS are presented and compared to leading-logarithm parton-shower Monte Carlo models. The predicted differences on the size of gluon- and quark-initiated jets are used to select samples to study the dynamics of the subprocesses.

INTRODUCTION

The internal structure of a jet depends mainly on the type of primary parton (quark or gluon) from which it originated and to a lesser extent on the particular hard scattering process. QCD predicts that (a) at sufficiently high transverse energy of the jet (E_T^{jet}), where fragmentation effects become negligible, the jet structure is driven by gluon emission from the primary parton; and (b) gluon jets are broader than quark jets due to the larger colour charge of the gluon. In the first part of this article, the measurements performed by ZEUS [1] to test the QCD prediction (a) are presented and compared to leading-logarithm parton-shower Monte Carlo models. The lowest non-trivial order contribution to the jet substructure is given by $\mathcal{O}(\alpha_s^2)$ calculations and, therefore measurements of jet substructure provide a stringest test of QCD beyond leading order (LO). The results of taking prediction (b) into account to test the dynamics of the subprocesses [2] are shown in the second part of this article.

At HERA, positrons of energy $E_e = 27.5$ GeV collide with protons of energy $E_p = 820$ GeV. The main source of jets is hard scattering in γp interactions in which a quasi-real photon ($Q^2 \approx 0$, where Q^2 is the virtuality of the photon) emitted by the positron beam interacts with a parton from the proton to produce two jets in the final state. In LO QCD, there are two processes which contribute to the jet production cross section: the resolved process (figure 1a) in which the

† Talk given at the *International Conference on the Structure and Interactions of the Photon* (PHOTON 2000), Ambleside, UK, August 26th – 31st, 2000.

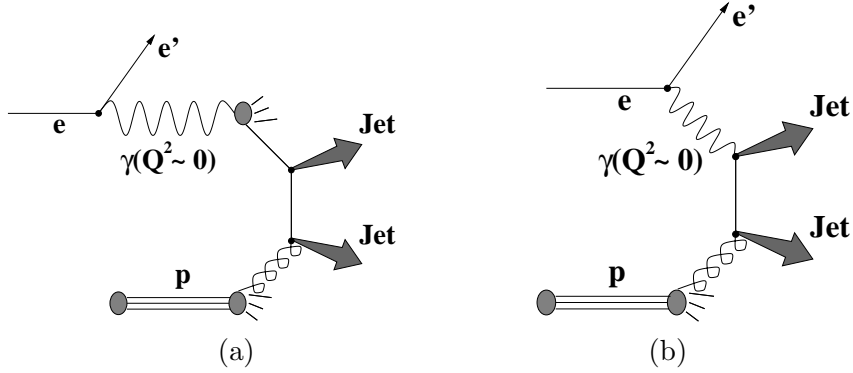


FIGURE 1. (a) Resolved- and (b) direct-photon processes.

photon interacts through its partonic content, and the direct process (figure 1b) in which the photon interacts as a point-like particle.

In the kinematic regime studied here, the dominant subprocesses are $q_\gamma g_p \rightarrow qg$ in resolved and $\gamma g \rightarrow q\bar{q}$ in direct. The kinematics of these processes are such that the majority of the jets in the region of pseudorapidity[‡] (η^{jet}) below 0 originate from quarks and the fraction of gluon-initiated jets increases as η^{jet} increases.

JET SUBSTRUCTURE

The internal structure of jets can be studied by means of the jet shape and the subjet multiplicity.

Jet shape

The differential jet shape is defined as the average fraction of the jet's transverse energy that lies inside an annulus in the pseudorapidity (η) - azimuth (φ) plane of radii $r \pm \Delta r/2$, where $r = \sqrt{(\Delta\eta)^2 + (\Delta\varphi)^2}$, concentric with the jet axis and is given by

$$\rho(r) = \frac{1}{N_{jets}} \cdot \frac{1}{\Delta r} \cdot \sum_{jets} \frac{E_T(r - \frac{\Delta r}{2}, r + \frac{\Delta r}{2})}{E_T(0, r = 1)},$$

where $E_T(r - \Delta r/2, r + \Delta r/2)$ is the transverse energy within the given annulus and N_{jets} is the total number of jets in the sample. The integrated jet shape is the average fraction of the jet's transverse energy that lies inside a cone in the $\eta - \varphi$ plane of radius r concentric with the jet axis,

[‡] The pseudorapidity is defined as $\eta = -\ln(\tan \frac{\theta}{2})$, where the polar angle θ is taken with respect to the proton beam direction. The ZEUS coordinate system is defined as right-handed with the Z -axis pointing in the proton beam direction, hereafter referred to as forward, and the X -axis horizontal, pointing towards the centre of HERA.

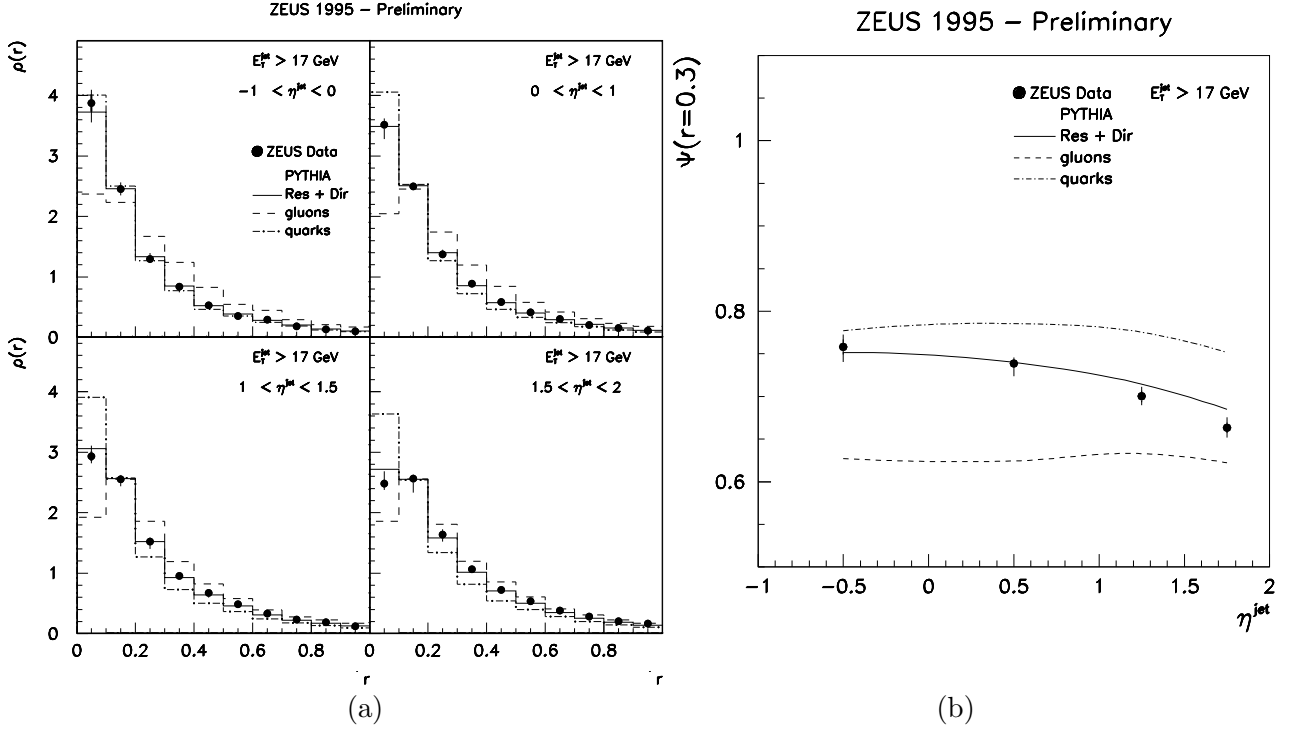


FIGURE 2. (a) Measured differential jet shape $\rho(r)$ vs. r (black dots). (b) Measured integrated jet shape $\psi(r = 0.3)$ vs. η^{jet} (black dots). PYTHIA Monte Carlo calculations are shown for comparison.

$$\psi(r) = \frac{1}{N_{jets}} \cdot \sum_{jets} \frac{E_T(r)}{E_T(r=1)}.$$

Measurements of the differential jet shape $\rho(r)$ have been performed by ZEUS [1] using an inclusive sample of jets. The jets have been identified using the longitudinally invariant k_T cluster algorithm [3] in the inclusive mode. The jets were required to have $E_T^{jet} > 17 \text{ GeV}$ and $-1 < \eta^{jet} < 2$. The measurements were performed in the kinematic region $0.2 < y < 0.85$, where y is the inelasticity variable, and $Q^2 \leq 1 \text{ GeV}^2$. Figure 2a shows $\rho(r)$ as a function of r in different regions of η^{jet} . The data show that the jets become broader as η^{jet} increases.

The solid histograms in figure 2a are calculations from the leading-logarithm parton-shower Monte Carlo PYTHIA [4]. The predictions, which include initial and final state QCD radiation, give a good description of the data. The comparison of the predictions for gluon- (dashed histograms) and quark-initiated (dot-dashed histograms) jets to the data shows that the measured jets are quark-like for $-1 < \eta^{jet} < 0$ and become increasingly more gluon-like as η^{jet} increases.

The quark and gluon content of the final state has been investigated in more detail by studying the η^{jet} dependence of the integrated jet shape at a fixed value of r [1]. Figure 2b shows $\psi(r)$ for $r = 0.3$ as a function of η^{jet} . The measured jet shape decreases with η^{jet} , i.e. the jets become broader as η^{jet} increases. The

comparison between the predictions of PYTHIA for gluon- and quark-initiated jets and the data shows that the broadening of the jets is consistent with an increasing fraction of gluon-initiated jets as η^{jet} increases.

Subject multiplicity

The application of the k_T cluster algorithm allows the study of the internal structure of the jets by means of jet-like objects (subjets) for which resummed QCD calculations are possible. Subjets are resolved within a jet by reapplying the k_T cluster algorithm until for every pair of particles the quantity

$$d_{ij} = \min(E_{Ti}, E_{Tj})^2 \cdot [(\eta_i - \eta_j)^2 + (\varphi_i - \varphi_j)^2]$$

is above $y_{cut} \cdot (E_T^{jet})^2$. The theoretical advantages of this observable are that safe observables can be defined at any order in perturbative QCD and resummed calculations are possible. Subjets are also a useful tool to investigate the colour dynamics. Finally, the uncertainties coming from hadronisation corrections are small when y_{cut} is not too small.

The mean subjet multiplicity $\langle n_{subjet} \rangle$ has been measured [1] for an inclusive sample of jets with $E_T^{jet} > 15$ GeV and $-1 < \eta^{jet} < 2$ in the kinematic region given by $0.2 < y < 0.85$ and $Q^2 \leq 1$ GeV². Figure 3a shows $\langle n_{subjet} \rangle$ as a function of y_{cut} . The predictions of PYTHIA and HERWIG [5], which include initial and final state QCD radiation, provide a good description of the data. The measured $\langle n_{subjet} \rangle$ for a fixed y_{cut} value of 0.01 (see figure 3b) increases as η^{jet} increases. The comparison to the predictions for gluon- and quark-initiated jets shows that the increase in $\langle n_{subjet} \rangle$ as η^{jet} increases is consistent with the predicted increase in the fraction of gluon-initiated jets. This result is consistent with the one obtained from the measurements of jet shapes.

SUBSTRUCTURE DEPENDENCE OF DIJET CROSS SECTIONS

The predictions of the Monte Carlo models for the jet shape and subjet multiplicity reproduce the data well and show the expected differences for quark- and gluon-initiated jets. Therefore, the Monte Carlo events have been used to devise a method to select samples enriched in quark- and gluon-initiated jets. The samples are selected by exploiting the QCD prediction that gluon-initiated jets should be broader than quark-initiated jets.

The predicted distributions of $\psi(r)$ for $r = 0.3$ and $\langle n_{subjet} \rangle$ for $y_{cut} = 0.0005$ for quark- and gluon-initiated jets are clearly different (see figure 4). A sample enriched in quark-initiated (“thin”) jets has been selected by requiring $\psi(r = 0.3) > 0.8$ and a sample enriched in gluon-initiated (“thick”) jets has been selected by requiring $\psi(r = 0.3) < 0.6$. Alternative samples to support the results obtained

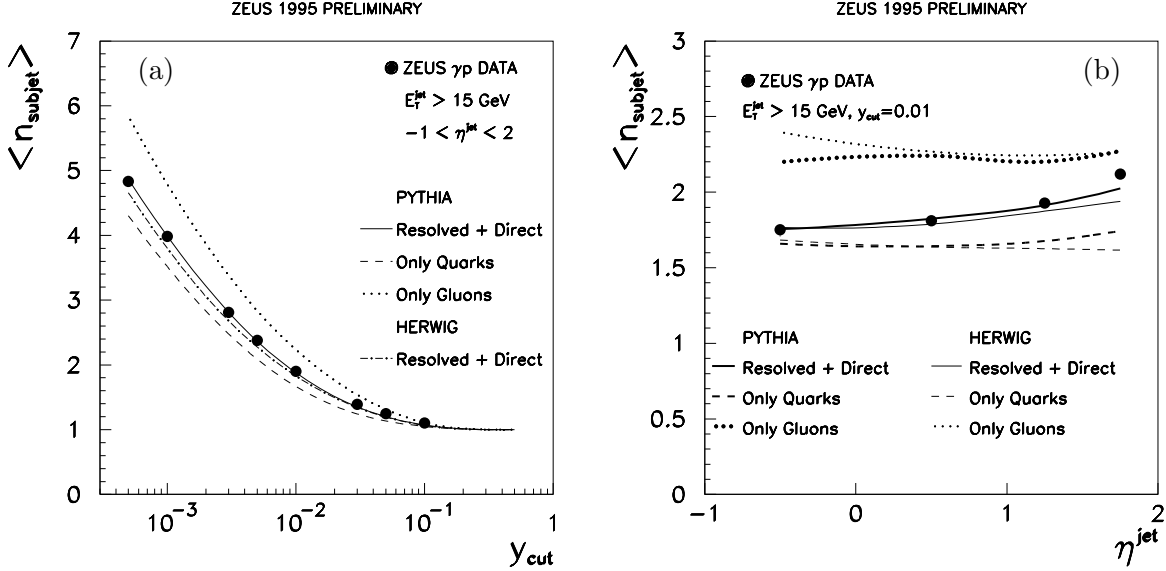


FIGURE 3. (a) Measured mean subjet multiplicity $\langle n_{\text{subjet}} \rangle$ vs. y_{cut} (black dots). (b) Measured mean subjet multiplicity $\langle n_{\text{subjet}}(y_{\text{cut}} = 0.01) \rangle$ vs. η^{jet} (black dots). PYTHIA and HERWIG Monte Carlo calculations are shown for comparison.

with the jet shape selection have been selected using the subjet multiplicity. Jets are called “thin” if $n_{\text{subjet}}(y_{\text{cut}} = 0.0005) < 4$ and the jets are called “thick” if $n_{\text{subjet}}(y_{\text{cut}} = 0.0005) \geq 6$.

Measurements of $d\sigma/d\eta^{\text{jet}}$

Using the jet shape selection into “thin” and “thick” jet samples, dijet cross sections have been measured [2] as a function of η^{jet} for events with at least two jets of $E_T^{\text{jet}} > 14$ GeV and $-1 < \eta^{\text{jet}} < 2.5$ in the kinematic region given by $0.2 < y < 0.85$ and $Q^2 \leq 1$ GeV². Figure 5 shows $d\sigma/d\eta^{\text{jet}}$ for “thick” and “thin” jets. The cross section for “thick” jets displays a very different shape than that of the “thin” jet sample: the η^{jet} distribution for the “thin” jet sample peaks at about 0.7, whereas the “thick” jet sample distribution peaks at $\eta^{\text{jet}} \approx 1.5$.

The predictions of PYTHIA and HERWIG (see figure 5a) give a good description of the data. The Monte Carlo distributions have been normalised to the total measured cross section of each type after applying the same jet shape selection as in the data. PYTHIA and HERWIG predict a similar parton content of the final state: the “thick” jet sample is composed of 15 – 17% of gg subprocesses in the final state, 54 – 58% of gq and 25 – 31% of qq . The “thin” jet sample contains 54 – 56% of qq , 41% of gq and 3 – 5% of gg . Therefore, the “thin” jet sample is indeed dominated by quark-initiated jets in the final state and the “thick” jet sample has a high content of gluon-initiated jets coming mainly from the final-state gluon of the subprocess $q_1 g_p \rightarrow qq$. The measurements are compared to the predictions of

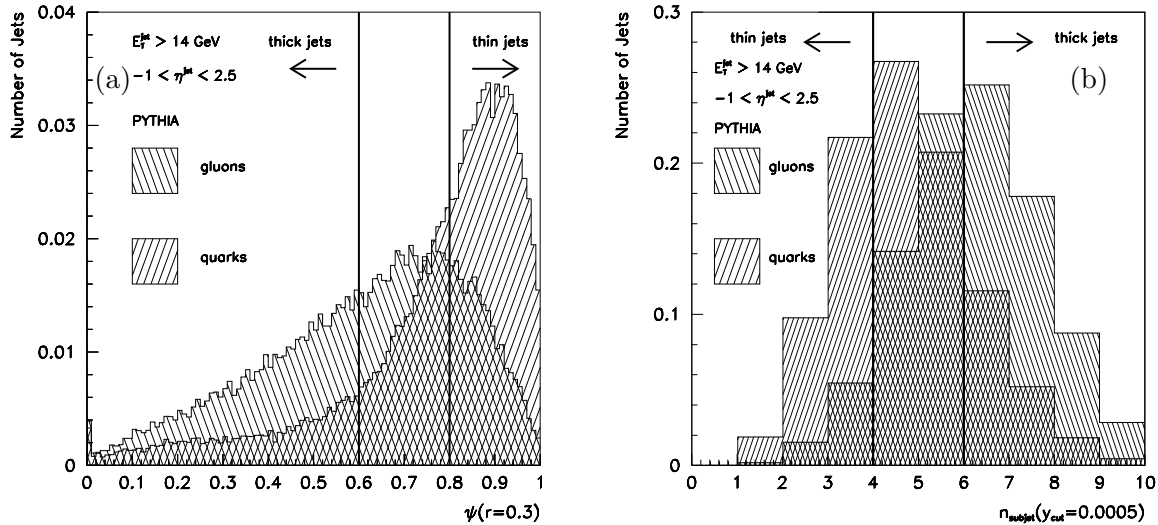


FIGURE 4. The predicted integrated jet shape $\psi(r = 0.3)$ (a) and subjet multiplicity $n_{subjet}(y_{cut} = 0.0005)$ (b) distributions at the hadron level for samples of gluon- and quark-initiated jets simulated using the program PYTHIA.

quark- and gluon-initiated jets with the same jet shape selection as for the data in figure 5b. A “thin”-quark jet sample gives a good description of the “thin” jet sample, whereas the “thin”-gluon jet sample peaks one unit of pseudorapidity higher. A sample of “thick”-quark jets alone cannot describe the “thick”-jet sample and a large content of gluon-initiated jets is needed to reproduce the shape of the data.

Measurements of $d\sigma/d \cos \theta^*$

The underlying parton dynamics is reflected in the distribution of the scattering angle in the dijet centre-of-mass system, θ^* . The $\cos \theta^*$ distribution is sensitive to the spin of the exchanged particle: for gluon exchange, the cross section is proportional to $(1 - |\cos \theta^*|)^{-2}$, whereas for quark exchange the cross section is proportional to $(1 - |\cos \theta^*|)^{-1}$. In a previous publication [6], the $|\cos \theta^*|$ distribution for resolved processes (which are dominated by subprocesses mediated by gluon exchange) was observed to rise more steeply than that of direct processes (which proceed via quark exchange) at high $|\cos \theta^*|$ values. In this analysis [2], samples of jets are selected according to their internal structure. This method provides a handle to better understand the dynamics of the subprocesses.

For samples of two “thick” or two “thin” jets, only the absolute value of $\cos \theta^*$ can be determined because the outgoing jets are indistinguishable. The dijet cross section as a function of $|\cos \theta^*|$ for samples of two “thick”-jet events and two “thin”-jet events has been measured for dijet invariant masses $M^{JJ} > 47$ GeV. The cross

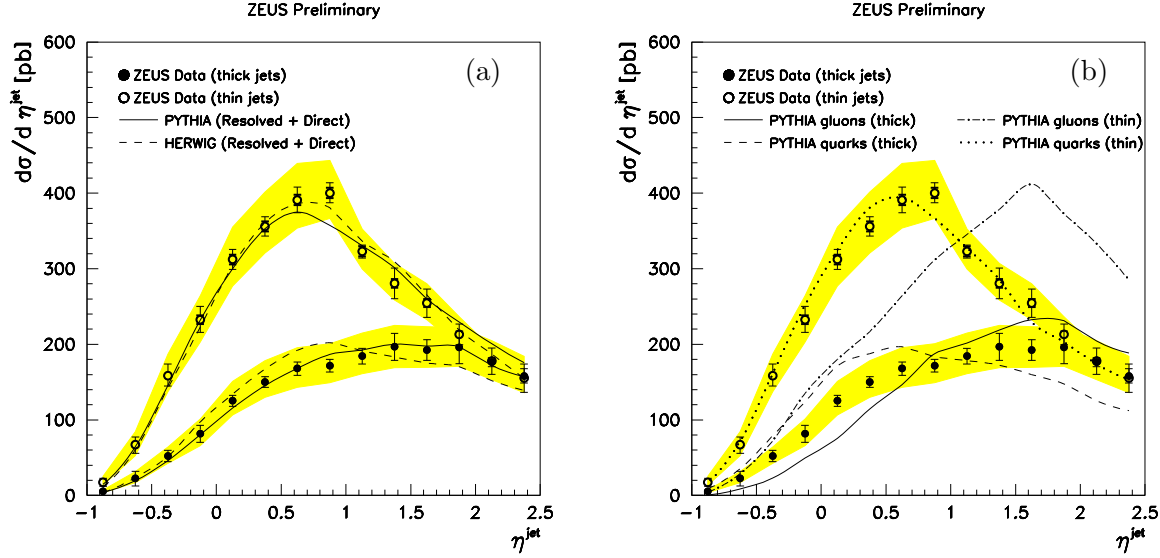


FIGURE 5. Measured $d\sigma/d\eta^{jet}$ for samples of “thick” (black dots) and “thin” (open circles) jets selected according to their shape. The thick error bars represent the statistical errors of the data, and the thin error bars show the statistical errors and uncorrelated systematic uncertainties added in quadrature. The shaded band displays the uncertainty due to the absolute energy scale of the jets. In (a) Monte Carlo calculations using PYTHIA and HERWIG for resolved- plus direct-photon processes and in (b) the predictions of PYTHIA for quark- and gluon-initiated jets are shown for comparison.

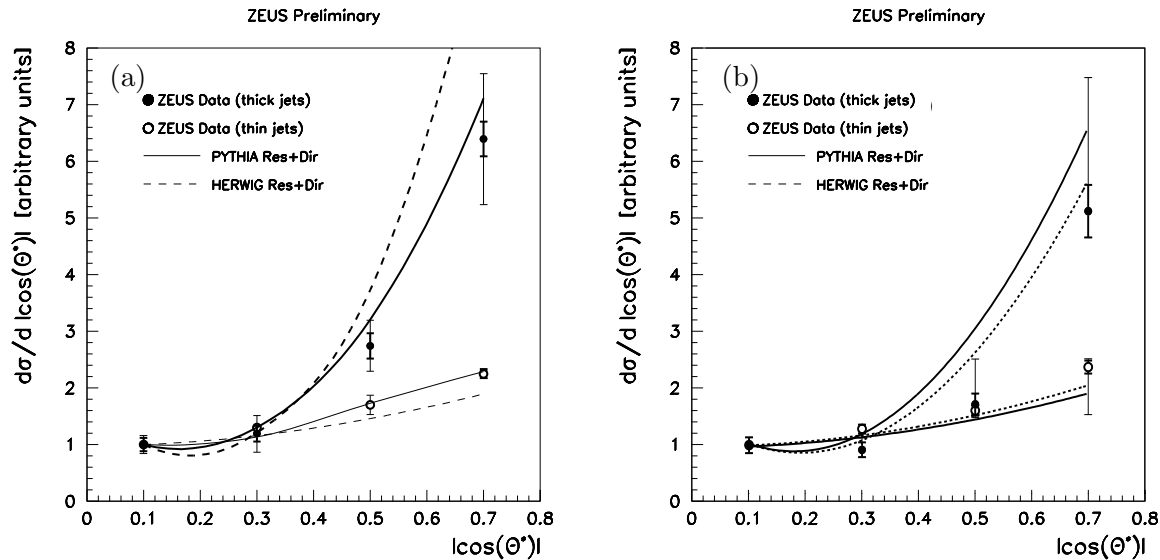


FIGURE 6. Measured $d\sigma/d|\cos\theta^*|$ for two “thick”-jet events (black dots) and two “thin”-jet events (open circles) selected according to their shape (a) or to their subjet multiplicity (b). PYTHIA and HERWIG Monte Carlo calculations are shown for comparison.

sections are presented in figure 6 and are normalised so as to have a value of unity at low $|\cos\theta^*|$ to study the difference in slope as $|\cos\theta^*| \rightarrow 1$. The $|\cos\theta^*|$ distribution for the two samples of dijet events increases as $|\cos\theta^*|$ increases, however they exhibit a different slope. For comparison, PYTHIA and HERWIG Monte Carlo predictions are shown in figure 6. The predictions have been also normalised so as to have a value of unity at low $|\cos\theta^*|$ and give a reasonable description of the shape of the data. The different slope observed in the data can be understood in terms of the dominant subprocesses in the two samples: the two “thick”-jet sample is dominated by subprocesses mediated by gluon exchange ($gg \rightarrow gg$ and $qg \rightarrow qg$) whereas the two “thin”-jet sample is dominated by subprocesses mediated by quark exchange ($\gamma g \rightarrow q\bar{q}$).

The sample of events with one “thick” jet and one “thin” jet allows a measurement of the unfolded $d\sigma/d\cos\theta^*$ cross section, since in this case the jets can be distinguished. Figure 7 shows the measured dijet cross section as a function of $\cos\theta^*$. The dijet angular distribution was measured with respect to the “thick” jet and shows a different behaviour on the negative and positive sides: the measured cross section at $\cos\theta^* = 0.7$ is more than two times larger than the one at $\cos\theta^* = -0.7$. The Monte Carlo models give a reasonable description of the shape of the measured $d\sigma/d\cos\theta^*$ (see figure 7). The measurements and the Monte Carlo calculations in figure 7 are normalised so as to have a value of unity at central values of $\cos\theta^*$ to study the difference in slope as $\cos\theta^* \rightarrow \pm 1$. The observed asymmetry is understood in terms of the dominant subprocess: $q_\gamma g_p \rightarrow qg$. The positive side is dominated by t -channel gluon exchange, whereas the negative side is dominated by u -channel quark exchange.

SUMMARY AND CONCLUSIONS

Measurements of jet shape and subjet multiplicity have been performed for inclusive jet samples with $E_T^{jet} > 15$ GeV and $-1 < \eta^{jet} < 2$ in the kinematic regime given by $0.2 < y < 0.85$ and $Q^2 \leq 1$ GeV². The measured jet shape broadens and the mean subjet multiplicity increases as η^{jet} increases. Leading-logarithm parton-shower Monte Carlo models with initial and final state QCD radiation give a good description of the data. The observed broadening of the jet shape and the increase in the mean subjet multiplicity as η^{jet} increases is consistent with an increase of the fraction of gluon jets.

The Monte Carlo models reproduce the measurements of the jet shape and subjet multiplicity and display the expected differences for quark- and gluon-initiated jets and allow the use of the jet shape and subjet multiplicity to select samples enriched in quark- and gluon-initiated jets to study the dynamics of the subprocesses. Measurements of the dijet cross section as a function of η^{jet} for samples of “thick” and “thin” jets show the expected behaviour for samples enriched in gluon- and quark-initiated jets. The $|\cos\theta^*|$ distribution for a two “thick”-jet sample displays a similar behaviour to the one expected for a sample enriched in processes

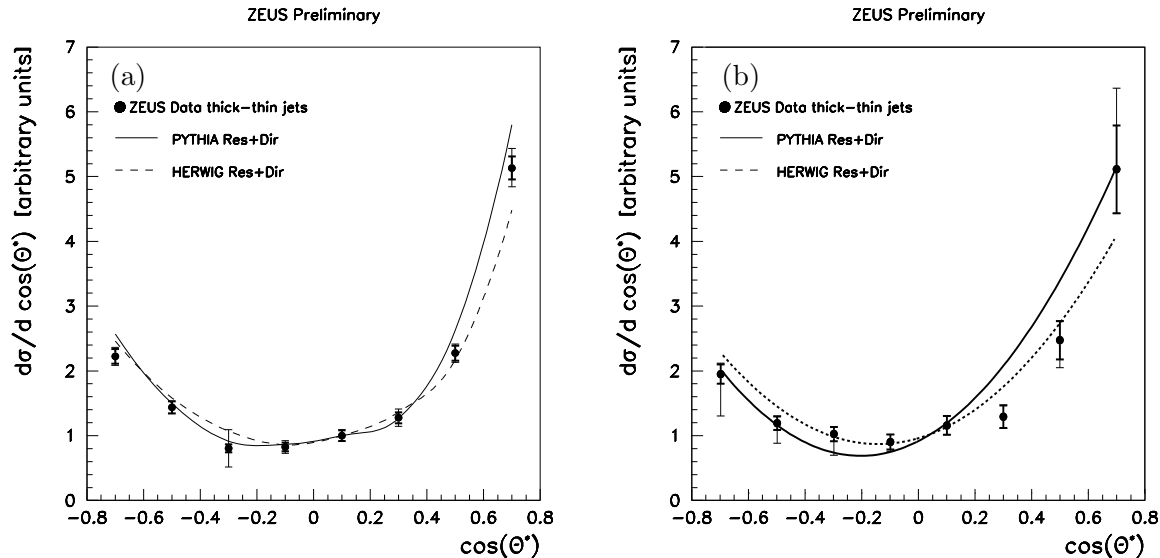


FIGURE 7. Measured $d\sigma/d\cos\theta^*$ for one “thick” jet and one “thin” jet in an event (black dots) selected according to their shape (a) or to their subjet multiplicity (b). PYTHIA and HERWIG Monte Carlo calculations are shown for comparison.

mediated by gluon exchange, whereas that for a two “thin”-jet sample shows a behaviour similar to a sample enriched in processes mediated by quark exchange. Finally, the $\cos\theta^*$ distribution for a sample of events with one “thick” and one “thin” jet exhibits a large asymmetry consistent with the expected dominance of t -channel gluon (u -channel quark) exchange as $\cos\theta^* \rightarrow +1(-1)$.

Acknowledgements. I would like to thank my colleagues from ZEUS for their help in preparing this report and the organisers of the conference for providing a warm atmosphere and hospitality.

REFERENCES

1. ZEUS Collaboration, “Measurements of Jet Substructure in Photoproduction at HERA”, paper 530, submitted to the International Europhysics Conference on HEP, Tampere (1999).
2. ZEUS Collaboration, “Substructure Dependence of Dijet Cross Sections in Photoproduction at HERA”, paper 424, submitted to the XXXth International Conference on HEP, Osaka (2000).
3. S. Catani *et al*, *Nucl. Phys.* **B** 406 (1993) 187; S.D. Ellis and D.E. Soper, *Phys. Rev.* **D** 48 (1993) 3160; M.H. Seymour, *Nucl. Phys.* **B** 513 (1998) 269.
4. H.-U. Bengtsson and T. Sjöstrand, *Comp. Phys. Comm.* 46 (1987) 43; T. Sjöstrand, *Comp. Phys. Comm.* 82 (1994) 74.
5. G. Marchesini *et al*, *Comp. Phys. Comm.* 67 (1992) 465.
6. ZEUS Collaboration, M. Derrick *et al*, *Phys. Lett.* **B** 384 (1996) 401.